

Dependence of single event upsets sensitivity of low energy proton on test factors in 65 nm SRAM

Yin-Yong Luo(罗尹虹), Feng-Qi Zhang(张凤祁), Xiao-Yu Pan(潘霄宇), Hong-Xia Guo(郭红霞), Yuan-Ming Wang(王圆明)

Citation: Chin. Phys. B . 2018, 27(7): 078501. **doi:** 10.1088/1674-1056/27/7/078501

Journal homepage: http://cpb.iphy.ac.cn; http://iopscience.iop.org/cpb

What follows is a list of articles you may be interested in

Closed-form breakdown voltage/specific on-resistance model using charge superposition technique for vertical power double-diffused metal-oxide-semiconductor device with high-κ insulator

Xue Chen(陈雪), Zhi-Gang Wang(汪志刚), Xi Wang(王喜), James B Kuo

Chin. Phys. B . 2018, 27(4): 048502. **doi:** 10.1088/1674-1056/27/4/048502

Detailed study of NBTI characterization in 40-nm CMOS process using comprehensive models

Yan Zeng(曾严), Xiao-Jin Li(李小进), Jian Qing(卿健), Ya-Bin Sun(孙亚宾), Yan-Ling Shi(石艳玲), Ao Guo(郭奥), Shao-Jian Hu(胡少坚)

Chin. Phys. B . 2017, 26(10): 108503. **doi:** 10.1088/1674-1056/26/10/108503

Improved high-frequency equivalent circuit model based on distributed effects for SiGe HBTs with CBE layout

Ya-Bin Sun(孙亚宾), Xiao-Jin Li(李小进), Jin-Zhong Zhang(张金中), Yan-Ling Shi(石艳玲)

Chin. Phys. B . 2017, 26(9): 098502. **doi:** 10.1088/1674-1056/26/9/098502

Superjunction nanoscale partially narrow mesa IGBT towards superior performance

Qiao-Qun Yu(喻巧群), Jiang Lu(陆江), Hai-Nan Liu(刘海南), Jia-Jun Luo(罗家俊), Bo Li(李博), Li-Xin Wang(王立新), Zheng-Sheng Han(韩郑生)

Chin. Phys. B . 2017, 26(3): 038502. **doi:** 10.1088/1674-1056/26/3/038502

Investigation on latch-up susceptibility induced by high-power microwave in complementary metal-oxide-semiconductor inverter

Yu-Hang Zhang(张宇航), Chang-Chun Chai(柴常春), Xin-Hai Yu(于新海), Yin-Tang Yang(杨银堂), Yang Liu(刘阳), Qing-Yang Fan(樊庆扬), Chun-Lei Shi(史春蕾)

Chin. Phys. B . 2017, 26(2): 028501. **doi:** 10.1088/1674-1056/26/2/028501

Dependence of single event upsets sensitivity of low energy proton on test factors in 65 nm SRAM*

Yin-Yong Luo(罗尹虹)†, Feng-Qi Zhang(张凤祁), Xiao-Yu Pan(潘霄宇), Hong-Xia Guo(郭红霞), and Yuan-Ming Wang(王圆明)

State Key Laboratory of Intense Pulsed Radiation Simulation and Effect, Northwest Institute of Nuclear Technology, Xi'an 710024, *China*

(Received 2 April 2018; revised manuscript received 2 May 2018; published online 25 June 2018)

In order to accurately predict the single event upsets (SEU) rate of on-orbit proton, the influence of the proton energy distribution, incident angle, supply voltage, and test pattern on the height, width, and position of SEU peak of low energy protons (LEP) in 65 nm static random access memory (SRAM) are quantitatively evaluated and analyzed based on LEP testing data and Monte Carlo simulation. The results show that different initial proton energies used to degrade the beam energy will bring about the difference in the energy distribution of average proton energy at the surface and sensitive region of the device under test (DUT), which further leads to significant differences including the height of SEU peak and the threshold energy of SEU. Using the lowest initial proton energy is extremely important for SEU testing with low energy protons. The proton energy corresponding to the SEU peak shifts to higher average proton energies with the increase of the tilt angle, and the SEU peaks also increase significantly. The reduction of supply voltage lowers the critical charge of SEU, leading to the increase of LEP SEU cross section. For standard 6-transitor SRAM with bit-interleaving technology, SEU peak does not show clear dependence on three test patterns of logical checkerboard 55H, all "1", and all "0". It should be noted that all the SEUs in 65 nm SRAM are single cell upset in LEP testing due to proton's low linear energy transfer (LET) value.

Keywords: low energy proton, energy distribution, tilt angle, supply voltage, test pattern

PACS: 85.30.De, 61.82.Fk, 21.60.Ka **DOI:** 10.1088/1674-1056/27/7/078501

1. Introduction

Proton is the main particle source that induces the single event effect (SEE) in electronics devices in space radiation environment. SEE is usually caused by the nuclear interaction of middle-high energy protons with material atoms. As the feature size of devices shrinks to nanometer scale, low energy protons (LEP) can give rise to single event upsets (SEU) with high cross section through direct ionization, which leads to a significant increase of on-orbit SEU rate, thus causing great concern from the researchers of radiation effect.

In 2007, Rodbell *et al.*[1] first reported LEP-induced SEU in 65 nm silicon on insulator (SOI) latch and static random access memory (SRAM) through direct ionization. Later, a large number of investigations about proton direct ionization (PDI)-induced SEE were carried out involving 90 nm to 25 nm SOI and body complementary metal oxide semiconductor (CMOS) latches, SRAMs, and flash memories.[2–17] The point was focused on the testing of SEU sensitivity due to PDI using LEP radiation sources. LEP SEUs are usually from single cell upset because of low linear energy transfer (LET) value of proton. As the feature size shrinks, LEP-induced MCUs were also observed in SRAM below 65 nm.[5–8] In order to acquire the height and the width of the SEU peak to accurately predict the PDI-induced SEU rate, the impact of proton incident angle and supply voltage on LEP SEU was further studied.[1–11] Because LEP SEU peak occurs in a narrow energy range, a small change in proton energy can induce large increase in SEU cross section, and the proton energy should be relatively monoenergetic to test the SEU cross section. However, monoenergetic protons below 1 MeV are difficult to acquire in practical proton testing. People usually use degraders with different thicknesses to get lower energy protons, so it is inevitable to introduce energy straggle. Moreover, the top overlayers or the back substrate of devices will also result in further energy straggle. A lot of debates have focused on how to make accurate characterization testing for PDI-induced SEE using degraded LEP beams with energy straggle.[7–14] Therefore, proton energies at the device surface and sensitive region must be estimated accurately using simulations based on the interaction between protons and material atoms in order to give the quantitative assessment.

In this paper, the influence of test factors on LEP SEU in 65 nm SRAM is investigated based on experiment with LEP accelerator and Monte Carlo simulations, including proton energy spectrum, proton incident angle, test pattern, and supply voltage. The effect of different test factors on LEP SEU peak is quantified and specified, and the root mechanism is revealed through combining the LEP testing data and the device process information with beam characteristics at the surface and sensitive region of device. This work has a practical significance for

*Project supported by the Major Program of the National Natural Science Foundation of China (Grant Nos. 11690040 and 11690043).

†Corresponding author. E-mail: luoyinhong@nint.ac.cn

© 2018 Chinese Physical Society and IOP Publishing Ltd

developing a more scientific proton single event test method and assessing the ability of hardness assurance of space PDI SEE in nanometer devices effectively.

2. Experimental details

The device under test (DUT) is SRAM fabricated in a 65 nm bulk CMOS process. The SRAM uses a standard 6-transistor cell. The nominal supply voltages are 1.2 V for core circuits. The thickness of the overlayers is about 5.7 μm with six copper-interconnection layers.

LEP SEU testing was performed in the vacuum at the EN tandem accelerator in the Institute of Heavy Ion Physics at Peking University. Proton energy of the accelerator can be continuously tuned from 1 MeV to 10 MeV. The protons with initial energy of 3 MeV and 1.2 MeV were degraded after passing through Al foils with different thicknesses, producing lower energy protons with a minimum energy of 0.20 MeV. Table 1 shows average proton energies at the DUT surface after 3 MeV and 1.2 MeV protons passing through Al foil. It should be noted that the initial proton energy is determined by adjusting the terminal voltage of EN tandem accelerator, so it is considered to be quasi-monoenergetic.

Table 1. Average proton energies at the DUT surface after 3 MeV and 1.2 MeV protons passing through Al foils with different thicknesses.

Average energy/MeV	The thickness of Al foil/μm	Average energy/MeV	The thickness of Al foil/μm
3	0	1.2	0
1.2	62	0.98	5
1.0	67	0.88	7
0.9	69	0.83	8
0.85	70	0.77	9
0.80	71	0.72	1
0.75	72	0.67	11
0.69	73	0.60	12
0.63	74	0.54	13
0.50	76	0.48	14
0.43	77	0.40	15
0.30	79	0.32	16
0.20	80	0.23	17

Due to the limitation of the minimum thickness of Al foil available, it is difficult to acquire completely identical average proton energy with different initial proton energy. Figures 1(a) and 1(b) show the energy distributions of several typical average proton energies after 1.2 MeV and 3 MeV protons traversing Al foil, respectively. SEU testing in 65 nm SRAM written with logical checkerboard 55H was carried out at 1.2 V, using a dynamic read mode during the irradiation period. DUTs were irradiated at normal incidence and tilt incidence of 60° along the well with the initial proton energy of 1.2 MeV. After acquiring the average proton energy corresponding to the peak of LEP SEU cross section with normal incidence, SEU testing was further performed at variable voltages ranging from nominal −10% (1.08 V) to +10% (1.32 V) with three test patterns of all "0", all "1", and logical checkerboard 55H.

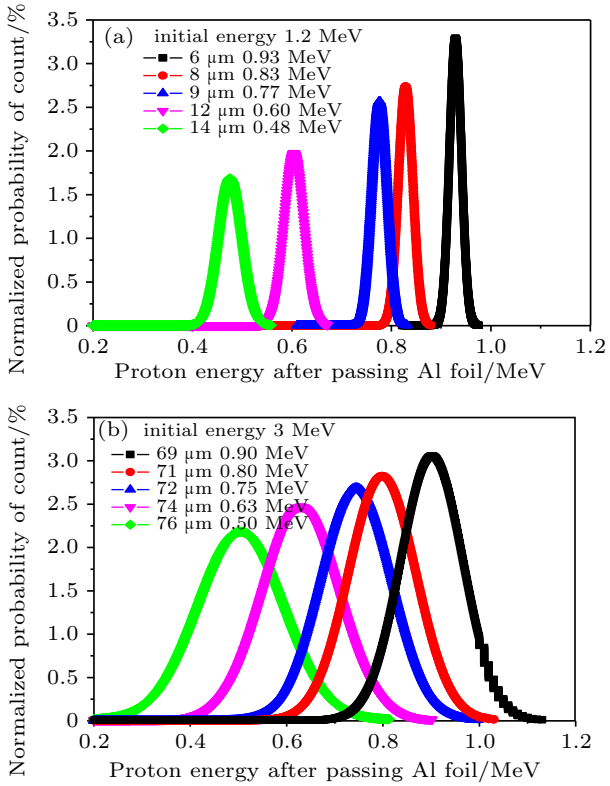


Fig. 1. (color online) Energy distributions of several typical average proton energies after 1.2 MeV and 3 MeV protons passing through Al foil. (a) The initial proton energy of 1.2 MeV; (b) the initial proton energy of 3 MeV.

3. Results and discussion

3.1. The dependence of LEP SEU on energy distribution of proton energy

Figure 2 shows proton single event upsets cross section versus proton energy with different initial proton energy. The *x*-axis is plotted as the average proton energies at the DUT surface after passing through Al foils. At proton energies below 1 MeV, a sharp increase is observed in SEU cross section. The increase is caused by upsets from LEP direct ionization.

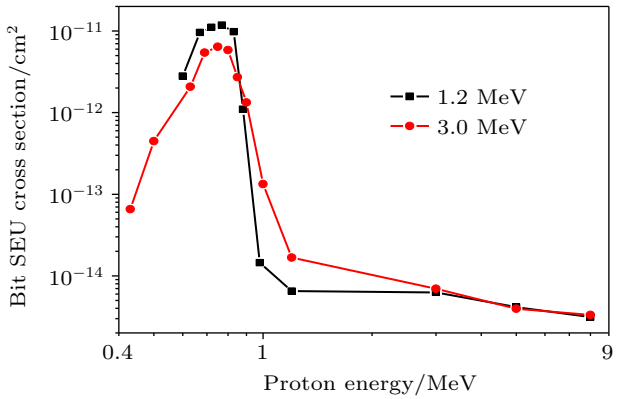


Fig. 2. (color online) Proton SEU cross section versus the average proton energy with different initial proton energies.

The position of the SEU peak is about between 0.65 MeV and 0.85 MeV, located at a narrow energy range of 0.2 MeV. The SEU peak values with the initial energy of 3 MeV and 1.2 MeV are 6.4×10^{-12} cm^2/bit and 1.18×10^{-11} cm^2/bit, respectively. Cross sections of SEU peak are both 3 orders of magnitude higher than that of 8 MeV protons, which indicates a transition from upsets due to nuclear events to direct ionization.

The maximum LET value of proton Bragg peak in silicon is 0.55 MeV·cm^2/mg at 55 keV protons. The LET value tends to decrease, and PDI capability weakens as proton energy on both sides of the Bragg peak increases or decreases (as shown in Fig. 3). The SEU LET threshold is around 0.28 MeV·cm^2/mg for 65 nm SRAM with the standard 6-transistor cells.[16] When the proton energy at the sensitive region is between 8 keV and 400 keV, proton LET is above 0.28 MeV·cm^2/mg, thus SEU will be caused. Nanoscale devices have multiple metal-interconnection layers. Protons will slow down when they pass through degrader and metallization layers. Not all protons lose the same amount of energy, which will introduce the energy straggle. Figure 4 presents energy distribution of 1.2 MeV protons with normal incidence after passing through 12 μm Al foil and metallization layers simulated with SRIM-2013.[8] SEU can occur as the proton energy at the DUT sensitive region is decreased between 8 keV and 400 keV.

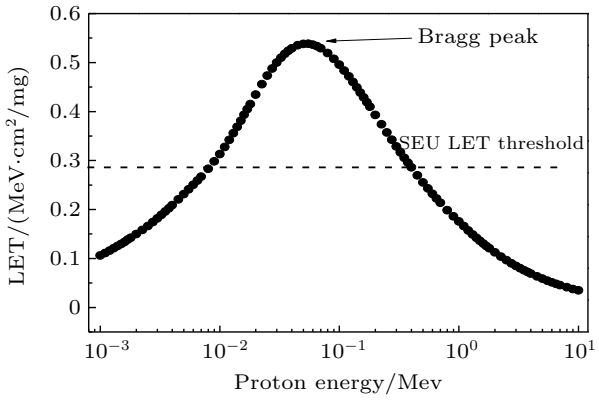


Fig. 3. (color online) Proton LET in silicon as a function of proton energy.

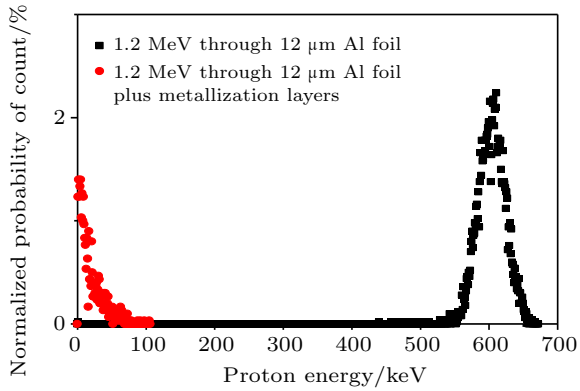


Fig. 4. (color online) Energy distributions of 1.2 MeV normal incidence beam after passing through the 12 μm Al foil and metallization layers.

Figure 5 plots proton LET as a function of penetration depth after protons penetrating through Al foils of different thicknesses and DUT multiple metallization layers with the initial proton energy of 1.2 MeV. The vertical dashed line corresponds to the position of DUT sensitive region. After 1.2 MeV protons passing through 14 μm Al foil, the average proton energy at the DUT surface is 0.48 MeV. The 0.48 MeV protons will lose all of their energy during traversing multiple metallization layers, and the range of protons is too short to reach the sensitive region, thus SEU cannot be caused.

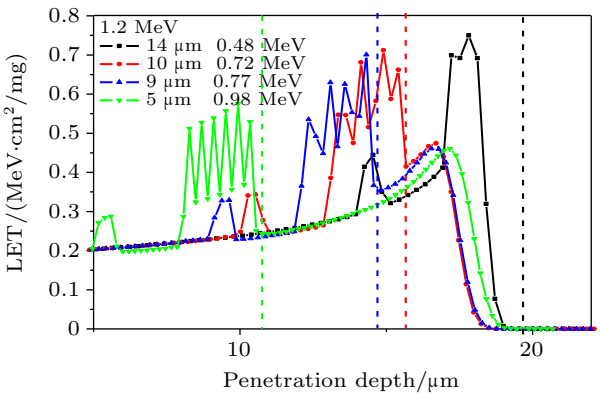


Fig. 5. (color online) Proton LET as a function of penetration depth after protons penetrating through Al foils of different thicknesses and DUT multiple metallization layers with the initial proton energy of 1.2 MeV.

With the decrease of the thickness of Al foil, the average proton energy incident at the DUT surface increases, the energy and number of protons reaching the sensitive region also increase accordingly. Figure 6(a) plots the normalized integral probability counts versus proton energy reaching the sensitive region after 1.2 MeV protons passing through aluminum foils of different thicknesses and metallization layers. Note that the rising edge or the peak of PDI Bragg curves with 9 μm and 10 μm Al foils just lies within the sensitive region, over 98.5% protons can get to the sensitive region, and the energy reaching the sensitive region is from 8 keV to 400 keV, which induce the highest SEU cross section and lead to the occurrence of the SEU peak.

As the thickness of Al foil further decreases, the average proton energy at the DUT surface continues to increase, and the proton energy reaching the sensitive region gets larger, even exceeding 400 keV. The LET value of some protons is below the SEU threshold, and the effective proton number between 8 keV and 400 keV which can cause SEU decreases. Taking 5 μm Al foil as an example, the average proton energy at the DUT surface is 0.98 MeV, and almost all the proton can reach the sensitive region. However, the energy of over 99% protons exceeds 500 keV and cannot bring about SEU. Only a tiny amount of protons below 400 keV can induce extra low SEU cross section in Fig. 2.

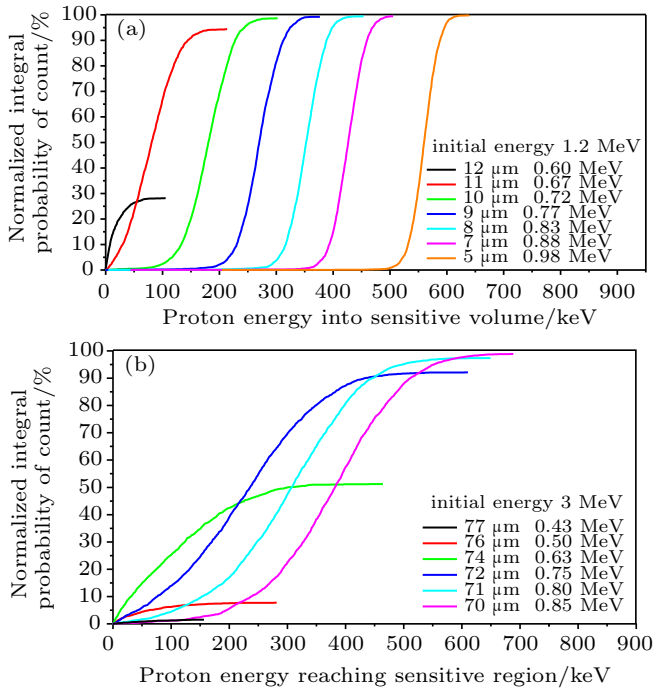


Fig. 6. (color online) Normalized integral probability count versus proton energy reaching the sensitive region after protons with different initial energies passing through Al foils of different thicknesses and metallization layers. (a) The initial proton energy of 1.2 MeV; (b) the initial proton energy of 3 MeV.

It can be seen that the SEU peak value with the initial proton energy of 3 MeV is 6.4×10^{-12} cm^2/bit, while the SEU peak value with the initial proton energy of 1.2 MeV is 1.18×10^{-11} cm^2/bit, which is about two times larger than that of 3 MeV. The average proton energy corresponding to the SEU peak in both cases is selected, a variety of information, including the energy distribution of the average proton energy, the energy and number of protons reaching the sensitive region, is analyzed. The average proton energy at the DUT surface corresponding to the SEU peak is 0.77 MeV with the initial proton energy of 1.2 MeV and 9 μm Al foil. The proton beam has a tight energy distribution with 31 keV standard deviation in Fig. 1(a). The dispersed degree of energy spread is smaller than 5%. Over 98.5% of the total protons can reach the sensitive region, and the proton energy is from 8 keV to 400 keV after protons passing through the metallization layers, which induces the highest SEU cross section. The average proton energy corresponding to the SEU peak is 0.75 MeV with the initial proton energy of 3 MeV and 72 μm Al foil. Using 72 μm Al foil makes a significant energy spread of proton beam at the DUT surface. The proton beam has a broadened energy distribution with 145 keV standard deviation in Fig. 1(b). The dispersed degree of energy spread approaches 20%. As the energy spread is severe, the energy distribution has a low energy tail. These lower energy protons have shorter range and cannot get to the sensitive region after protons traversing the metallization layers, indicating flux attrition. Those higher energy protons in energy distribution can reach the sensitive region, but the proton energy is over 400 keV and LET value is too low to cause SEU. Only 85% protons in Fig. 6(b) can reach the sensitive region, and the proton energy is between 8 keV and 400 keV. The effective proton number is obviously less than that with the initial proton energy of 1.2 MeV in Fig. 6(a), so the SEU peak cross section is lower than that of 1.2 MeV protons.

It can be seen further in Fig. 2 that not only the SEU peak value decreases, but the energy threshold of SEU also decreases with the initial energy of 3 MeV compared with that of 1.2 MeV. When the initial proton energy is 3 MeV, there is still a low SEU cross section at the average proton energy of 0.43 MeV incident at the DUT surface. However, the average energy below 0.6 MeV cannot induce SEU with the initial proton energy of 1.2 MeV. Combined with the energy distribution in Fig. 1(b), the average energy of 0.43 MeV with the initial proton energy of 3 MeV has a wide energy distribution with 190 keV standard deviation, and the dispersed degree of energy spread reaches 44%. The 0.43 MeV protons themselves do not have enough energy to traverse the metallization layers and get to the DUT sensitive region. But a small quantity of protons above 0.6 MeV in the high energy tail of energy distribution can reach the sensitive region to induce a low SEU cross section (as shown in Fig. 2). The different initial proton energy brings energy distribution difference of average proton energy at the DUT surface, which leads to obvious differences in the height of SEU peak and the threshold energy of SEU.

3.2. The dependence of LEP SEU on proton incident angle

Generally, proton SEU testing is carried out only at normal incidence, since it is believed that the proton incident angle has no impact on proton SEU. When SEUs are from PDI, the dependence of SEU on proton incident angle will show different characteristic. Figure 7 plots the proton SEU cross section versus the average proton energy at normal incidence and 45° tilt incidence with the initial proton energy of 1.2 MeV. The data of Fig. 7 are plotted as effective SEU cross sections, meaning that SEU cross section is scaled by $1/\cos(\text{angle})$ to account for the reduction in flux as the incident angle is changed. With the increase of the tilt angle, the SEU peak shifts to higher average proton energy. The SEU peak is located between 0.80 MeV and 1 MeV. The SEU peak value with tilt angle of 45° is 2.72×10^{-11} cm^2/bit and is two times higher than that with normal incidence.

Figure 8 presents proton LET as a function of penetration depth after protons with different average energies penetrating through DUT multiple metallization layers at 45° tilt incidence. Tilt incidence increases protons penetration length through DUT metallization layers, thus higher energy protons are required to penetrate the effectively thicker materials. Only when the average proton energy is between 0.80 MeV and 1 MeV, the peak and rising edge of PDI Bragg curves lie

within the sensitive region, causing the highest SEU cross section. Moreover, the increase in the penetration length through the DUT sensitive region increases the equivalent LET value, leading to the increase in SEU peak cross section compared with that at normal incidence.

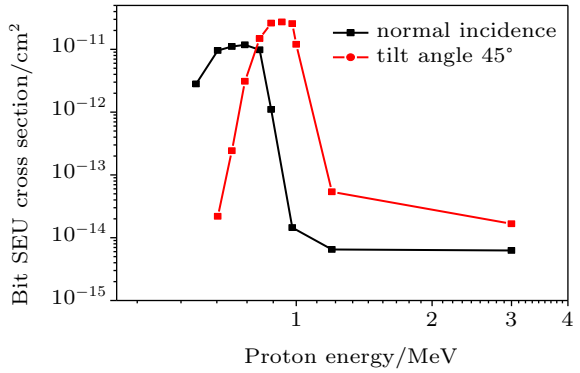


Fig. 7. (color online) Proton SEU cross section versus the average proton energy with the normal incidence and tilt incidence of 45° with the initial proton energy of 1.2 MeV.

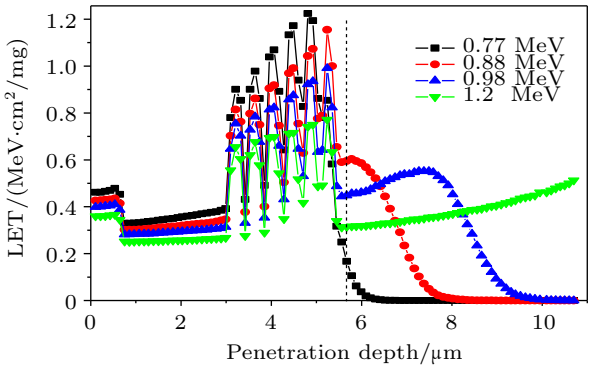


Fig. 8. (color online) Proton LET as a function of penetration depth after protons with different average energies penetrating through DUT multiple metallization layers with tilt angle of 45°.

As the energy of the incident proton at the DUT surface increases to 1.2 MeV, the energy of the vast majority of protons reaching the sensitive region exceeds 400 keV. Only very few protons between 8 keV and 400 keV induce low cross section SEU through direct ionization, but the SEU cross section is still one order of magnitude higher than that at normal incidence. This difference comes from different proton physical mechanism. The proton energy reaching the sensitive region exceeds 700 keV after 1.2 MeV protons passing through DUT multiple metallization layers at normal incidence. Proton LET is too low to cause SEU, only recoil nuclei coming from elastic collision of protons with material atoms can induce SEU. Because the reaction cross section of elastic collision is much smaller than that of direct ionization, SEU cross section of 1.2 MeV protons at normal incidence is much smaller than that at tilt incidence as well.

The logical addresses and data of flipped memory cells are recorded at each test cycle. Through building the relationship between the logical addresses and the physical addresses, SEU physical bitmap can be acquired. The uniformity of proton beam can be judged based on SEU physical distribution from a period of irradiation time, and relative locations of flipped memory cells are analyzed in order to identify if multiple cells upsets (MCU) occur. Figure 9 shows SEU physical bitmap from several test cycles at 45° tilt incidence of 0.88 MeV protons. Even at the proton energy corresponding to SEU peak, low energy proton cannot cause double MCU or higher order of MCU in 65 nm SRAM due to low PDI LET. All the SEUs come from single cell upset.

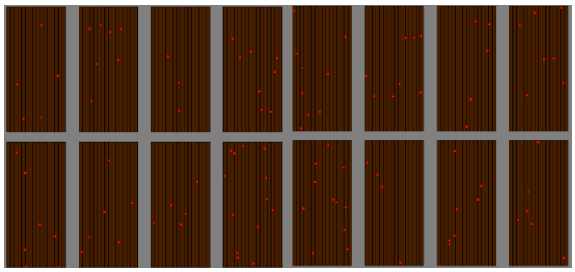


Fig. 9. (color online) SEU physical bitmap from several test cycles at tilt incidence of 0.88 MeV protons.

3.3. The dependence of LEP SEU on test pattern and supply voltage

Figure 10 plots LEP SEU peak cross section versus supply voltage with three test patterns in 65 nm SRAM. SEU peak value increases obviously with the decrease of supply voltage. With the memory cells written with 55H, SEU peak cross section increases by an order of magnitude, from 2.67×10^{-12} cm^2/bit to 3.5×10^{-11} cm^2/bit, while supply voltage decreases from 1.32 V to 1.08 V, which will make on-orbit SEU rate increase sharply. Lowering the voltage leads to the reduction of noise margin and SEU critical charge in SRAM. When the proton energy is the same, only the protons incident at the center of off-state drain region can deposit enough charge to induce SEU at higher voltage. With the decrease of the voltage, the protons incident at the outer area of off-state drain can also deposit an amount of charge to trigger SEU. Therefore, SEU sensitive area, i.e., SEU cross section increases at lower voltage.

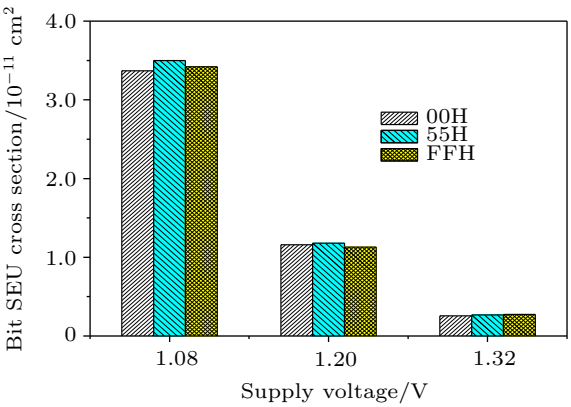


Fig. 10. (color online) Low energy proton SEU peak cross section versus supply voltage with three test patterns in 65 nm SRAM.

The relative locations of SEU sensitive nodes are usually affected by test patterns filled into memory cells due to the design of device layout, so SEU cross section, MCU percentage, and topological patterns would also be influenced. But SEU cross sections with three different test patterns of logical checkerboard 55H, all "1", and all "0" have no clear difference at the same voltage in Fig. 10. Owing to the use of bit-interleaving technology in 65 nm SRAM, the successive bits of logical words are separated, all memory cells are divided to large regions with "1" and "0" when the memory cells are filled with 55H. The width of these regions is 16 cells according to the layout design. All the cells are the state of "1" or "0" when filled with all "1" or all "0" pattern. Actually the position of the adjacent sensitive nodes with all "0" is the same as all "1", so there is no physical difference of sensitive nodes among these patterns of logical checkerboard, all "1" and all "0". Therefore, LEP peak SEU with three test patterns is the same as shown in Fig. 10.

4. Conclusion

Low energy protons SEE in nanometer devices have attracted more and more attention. In order to get the height and the width of the PDI SEU peak with LEP radiation sources to predict proton space SEU rate, the dependence of LEP SEU peak on test factors including proton energy distribution, incident angle, supply voltage, and test pattern was quantitatively evaluated and analyzed based on LEP testing data and Monte Carlo simulation. The results indicate that using the lowest initial energy allows the minimum thickness degrader used in LEP testing, which minimize the energy spread of proton beam striking the DUT. It is recommended that the dispersed degree of energy spread incident at the DUT surface should be smaller than 10% in order to get accurate SEU peak to predict on-orbit SEU-rate.

As the feature size of devices shrinks and the critical charge of SEU decreases, LEP SEU will also caused by low energy protons above 400 keV. It can be foreseen that the width of LEP SEU peak will further increase, and MCU will also occur, thus proton SEU rate will increase accordingly. LEP SEUs exhibit a strong dependence on the incident angle and supply voltage. The increase of protons incident angle and the reduction of DUT supply voltage will lead to the increase of SEU peak. The influence of test pattern on LEP SEU peak depends on the device layout design. For standard 6-transitor SRAM with bit-interleaving technology, LEP SEU peak has no clear dependence on three test patterns of 55H, all "1", and all "0". With the above study, it can be known that the impact of various test factors on LEP SEU must be considered carefully when predicting the proton SEU rate, which is different from traditional prediction method of proton SEU rate.

References

[1] Rodbell K P, Heidel D F, Tang H H K, Gordon M S, Oldiges P and Murray C E 2007 *IEEE Trans. Nucl. Sci.* **54** 2474

[2] Lawrence R K, Ross J F, Haddad N F, Reed R A and Albrecht D R 2009 *Proc. IEEE Radiat. Eff. Data Workshop Rec.*, Jul 20–24, 2009, Quebec, Canada, p. 123

[3] Dodds N A, Martinez M J, Dodd P E, *et al.* 2015 *IEEE Trans. Nucl. Sci.* **62** 2440

[4] Rodbell K P, Gordon M S, Stawiasz K G, Oldiges P, Lilja K and Turowski M 2017 *IEEE Trans. Nucl. Sci.* **64** 999

[5] Heidel D F, Marshall P W, Pellish J A, Rodbell K P, LaBel K A, Schwank J R, Rauch S E, Hakey M C, Berg M D, Castaneda C M, Dodd P E, Friendlich M R, Phan A D, Seidleck C M, Shaneyfelt M R and Xapsos M A 2009 *IEEE Trans. Nucl. Sci.* **56** 3499

[6] Seifert N, Gill B, Pellish J A, Marshall P W and LaBel K A 2011 *IEEE Trans. Nucl. Sci.* **58** 2711

[7] Weulersse C, Miller F, Alexandrescu D, Schaefer E and Gaillard R 2011 *Proc. Eur. Conf. Radiation and Its Effects on Components Systems*, Sep 19–23, 2011, Sevilla, Spain, p. 291

[8] Pellish J A, Marshall Paul W, Rodbell K P, Gordon M S, LaBel K, Schwank J R, Dodds N A, Castaneda C M, Berg M D, Kim H S, Phan A M and Seidleck C M 2014 *IEEE Trans. Nucl. Sci.* **61** 2896

[9] Cannon E H, Cabanas-Holmen M, Wert J, Amort T, Brees R, Koehn J, Meaker B and Normand E 2010 *IEEE Trans. Nucl. Sci.* **57** 3493

[10] Dodds N A, Dodd P E, Shaneyfelt M R, Sexton F W, Martinez M J, Black J D, Marshall P W, Reed R A, McCurdy M W, Weller R A, Pellish J A, Rodbell K P and Gordon M S 2015 *IEEE Trans. Nucl. Sci.* **62** 2822

[11] Ye B, Liu J, Wang T S, Liu T Q, Maaz K, Luo J, Wang B, Yin Y N, Ji Q G, Sun Y M and Hou M D 2017 *Nucl. Instrum. Methods Phys. Res. Sect. B* **406** 443

[12] Sierawski B D, Pellish J A, Reed R A, Schrimpf R D, Warren K M, Weller R A, Mendenhall M H, Black J D, Tipton A D, Xapsos M A, Baumann R C, Xiaowei D, Campola M J, Friendlich M R, Kim H S, Phan A M and Seidleck C M 2009 *IEEE Trans. Nucl. Sci.* **56** 3085

[13] Heidel D F, Marshall P W, LaBel K A, Schwank J R, Rodbell K P, Hakey M C, Berg M D, Dodd P E, Friendlich M R, Phan A D, Seidleck C M, Shaneyfelt M R and Xapsos M A 208 *IEEE Trans. Nucl. Sci.* **55** 3394

[14] He A L, Guo G, Chen L, Shen D J, Ren Y, Liu J C, Zhang Z C, Cai L, Shi S T, Wang H, Fan H, Gao L J and Kong F Q 2014 *At. Energy Sci. Technol.* **48** 2364 (in Chinese)

[15] Haddad N F, Kelly A T, Lawrence R K, Bin L, Rodgers J C, Ross J F, Warren K M, Weller R A, Mendenhall M H and Reed R A 2011 *IEEE Trans. Nucl. Sci.* **58** 975

[16] Luo Y H, Zhang F Q, Wang Y P, Wang Y M, Guo X Q and Guo H X 2016 *Acta Phys. Sin.* **65** 068501 (in Chinese)

[17] Bagatin M, Gerardin S, Paccagnella A, Visconti A, Virtanen A, Kettunen H, Costantino A, Ferlet-Cavrois V and Zadeh A 2017 *IEEE Trans. Nucl. Sci.* **64** 464

[18] SRIM2013-The Stopping and Range of Ions in Matter. [Online]. Available: http://www.srim.org